american physiological society

JNP JOURNAL OF NEUROPHYSIOLOGY

J Neurophysiol 125: 1223–1235, 2021.
First published January 27, 2021; doi:10.1152/jn.00317.2019

RESEARCH ARTICLE

Sensory Processing

Interjoint coupling of position sense reflects sensory contributions of biarticular muscles

Troy M. Herter,[1,2] Isaac Kurtzer,[1,3] Lauren Granat,[3] Frédéric Crevecoeur,[1,4,5] Sean P. Dukelow,[1,6,7] and Stephen H. Scott[1,8]

[1]*Center for Neuroscience Studies, Queen's University, Kingston, Ontario, Canada;* [2]*Department of Exercise Science, University of South Carolina, Columbia, South Carolina;* [3]*Department of Biomedical Sciences, New York Institute of Technology, New York City, New York;* [4]*Institute of Communication Technologies, Electronics and Applied Mathematics, Université Catholique de Louvain, Louvain-la-Neuve, Belgium;* [5]*Institute of Neuroscience, Université Catholique de Louvain, Louvain-la-Neuve, Belgium;* [6]*Hotchkiss Brain Institute, University of Calgary, Calgary, Alberta, Canada;* [7]*Department of Clinical Neurosciences, University of Calgary, Calgary, Alberta, Canada; and* [8]*Department of Biomedical and Molecular Sciences, Queen's University, Kingston, Ontario, Canada*

Abstract

Perception of limb position and motion combines sensory information from spindles in muscles that span one joint (monoarticulars) and two joints (biarticulars). This anatomical organization should create interactions in estimating limb position. We developed two models, one with only monoarticulars and one with both monoarticulars and biarticulars, to explore how biarticulars influence estimates of arm position in hand (*x*, *y*) and joint (*shoulder, elbow*) coordinates. In hand coordinates, both models predicted larger medial-lateral than proximal-distal errors, although the model with both muscle groups predicted that biarticulars would reduce this bias. In contrast, the two models made significantly different predictions in joint coordinates. The model with only monoarticulars predicted that errors would be uniformly distributed because estimates of angles at each joint would be independent. In contrast, the model that included biarticulars predicted that errors would be coupled between the two joints, resulting in smaller errors for combinations of flexion or extension at both joints and larger errors for combinations of flexion at one joint and extension at the other joint. We also carried out two experiments to examine errors made by human subjects during an arm position matching task in which a robot passively moved one arm to different positions and the subjects moved their other arm to mirror-match each position. Errors in hand coordinates were similar to those predicted by both models. Critically, however, errors in joint coordinates were only similar to those predicted by the model with monoarticulars and biarticulars. These results highlight how biarticulars influence perceptual estimates of limb position by helping to minimize medial-lateral errors.

NEW & NOTEWORTHY It is unclear how sensory information from muscle spindles located within muscles spanning multiple joints influences perception of body position and motion. We address this issue by comparing errors in estimating limb position made by human subjects with predicted errors made by two musculoskeletal models, one with only monoarticulars and one with both monoarticulars and biarticulars. We provide evidence that biarticulars produce coupling of errors between joints, which help to reduce errors.

muscle spindles; musculoskeletal; proprioception

INTRODUCTION

Proximal joints of the upper and lower limbs are spanned by several muscles, including some that only span one joint (monoarticulars) and others that cross two joints (biarticulars). The presence of biarticulars leads to coupling of motor patterns between joints, such that biarticulars are normally recruited during production of torques at a single joint (1–6).

Correspondence: S. H. Scott (steve.scott@queensu.ca).
Submitted 20 May 2019 / Revised 6 January 2021 / Accepted 6 January 2021

For example, the biceps are biarticulars that generate flexor torques at both the shoulder and elbow. When the biceps are recruited to generate elbow flexor torques, they also generate shoulder flexor torques that are countered by recruiting shoulder extensor muscles. Thus, shoulder extensor muscles tend to be active when one generates shoulder extensor or elbow flexor torques, and elbow extensor muscles tend to be active when one generates elbow extensor or shoulder flexor torques. Correspondingly, shoulder and elbow flexor muscles exhibit covariation when the long head of the triceps is recruited to generate elbow extensor or shoulder extensor torques.

Far less is known on how the anatomical organization of muscles influences proprioception. We know that all muscles are richly endowed with muscle spindles (7) and perception of joint angle and rotation is influenced by the stretch of all muscles that cross a joint (8, 9). Although spindle afferents from monoarticulars provide a direct measure of joint angle and rotation, the relationship between spindle afferent activities and proprioception is far more complex due to the presence of biarticulars. Consider the predictions of two anatomical organizations of the arm, one with only monoarticulars (Fig. 1*A*, *left*) and one that also includes biarticulars with similar mechanical actions to the biceps and long head of the triceps (Fig. 1*A*, *right*). The predicted influence of biarticulars on estimates of limb position is particularly evident in joint (*shoulder, elbow*) coordinates. In the first anatomical organization, monoarticulars only respond to rotations of the spanned joint, thus their activities are aligned with the primary axes in Cartesian joint (*shoulder, elbow*) coordinates (Fig. 1, *B* and *C*, magenta and orange arrows, *left*). Importantly, because afferent signals are not coupled between joints, sensory resolution is similar in all directions and estimates of limb position exhibit circular distributions of errors in Cartesian joint coordinates (Fig. 1*D*, *left*). In contrast, biarticulars in the second anatomical organization respond to flexion at both joints and extension at both joints (Fig. 1*B*, cyan arrow, *right*) but are minimally responsive when flexion at one joint is coupled with extension at the other joint (Fig. 1*C*, absent cyan arrow, *right*). This nonorthogonal organization provides biased information, thus estimates of limb position in Cartesian joint coordinates exhibit smaller errors in the first and third quadrants than in the second and fourth quadrants (Fig. 1*D*, *right*). Perhaps surprisingly, and not as interesting, the predicted influence of biarticulars on estimates of limb position is less obvious in Cartesian hand (*x, y*) coordinates because both anatomical organizations predict similar, elliptical distributions of errors (Fig. 1*E*).

Two theoretical studies have examined how the presence of biarticulars should influence perceptual estimates of limb position (10) and movement (11). Although these studies found that biarticulars should improve estimates of limb position and movement, neither of these studies directly compared their theoretical predictions with empirical data. In fact, we are only aware of one study that has provided empirical evidence that biarticulars influence proprioception (12). This study showed that thresholds for correctly discriminating the direction of passive wrist rotation increased (i.e., decreased perception) when the elbow was concurrently rotated in the opposite

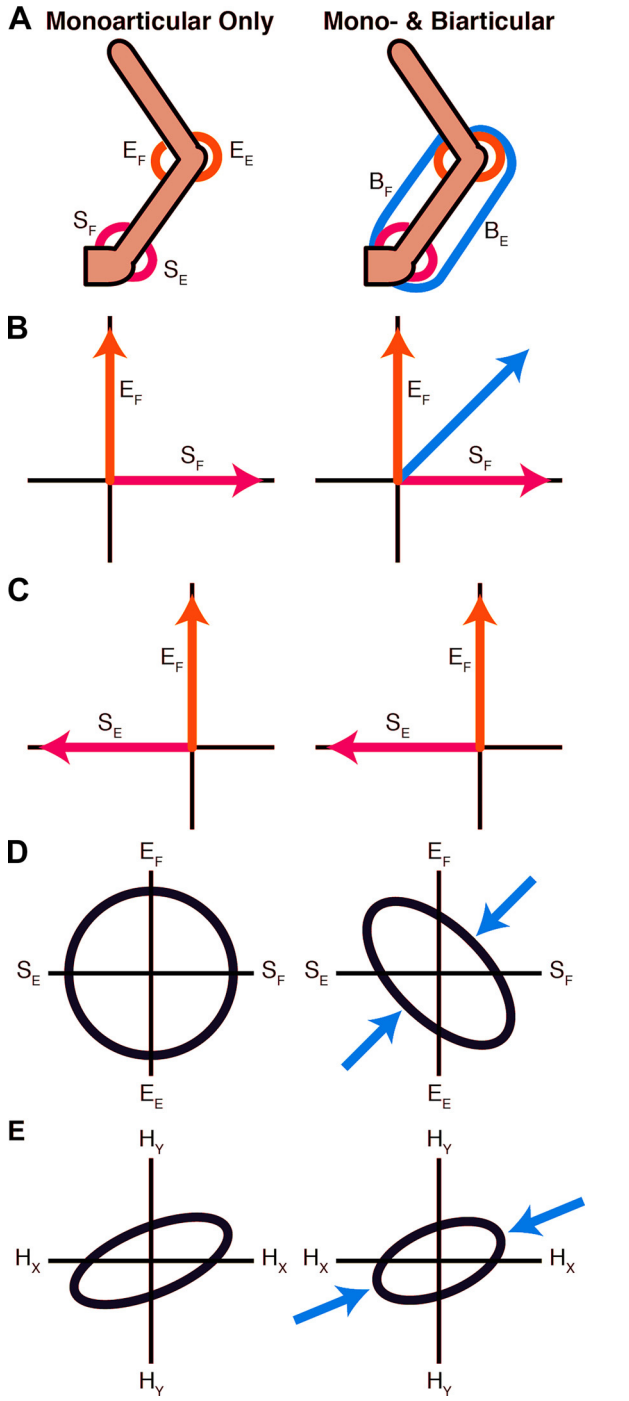

Figure 1. Conceptual framework. *A*: two anatomical organizations of the arm, one with monoarticulars only (*left*) and one with both monoarticulars and biarticulars (*right*). *B* and *C*: anatomical actions of shoulder monoarticulars (magenta lines), elbow monoarticulars (orange lines), and biarticulars (cyan lines) in Cartesian joint (*shoulder, elbow*) coordinates. Anatomical actions of the biarticulars couple flexion of both the shoulder and elbow (*B, right*) or extension of both the shoulder and elbow (not illustrated). Muscle spindles respond to joint rotations that involve the anatomical action of their respective muscle. *D* and *E*: distributions of errors predicted by each model in joint (*shoulder, elbow*) coordinates (*D*) and hand (*x, y*) coordinates (*E*). Biarticulars lead to smaller errors for rotations that couple flexion of both shoulder and elbow or extension of both the shoulder and elbow (*D,* cyan arrows). Biarticulars also lead to smaller errors for medial-lateral changes in hand position (*E,* cyan arrows). E_E, elbow extension; E_F, elbow flexion; H_X, hand-X; H_Y, hand-Y; S_F, shoulder flexion; S_E, shoulder extension.

direction. The study also observed increased thresholds (i.e., decreased perception) for correctly discriminating the direction of passive elbow rotation when the wrist was concurrently rotated in the opposite direction. Overall, these findings suggest that the biarticulars were responsible for the decreased perception of joint rotations because rotating the adjacent joint in the opposite direction would have minimized changes in length of the biarticulars, which cross the elbow and wrist on the same side.

Here, we use two musculoskeletal models, one with only monoarticulars (MO model) and one with both monoarticulars and biarticulars (MB model), to explore how the presence of biarticulars should influence estimates of limb position by coupling errors between the two joints. In addition, we directly compare the theoretical predictions from our models with empirical data from human subjects who performed an arm position matching task in which an upper-limb robot passively moved one arm to different positions and the subjects actively moved their opposite arm to mirror-match each position. In two separate experiments, one with many subjects but few trials (*experiment 1*) and one with few subjects but many trials (*experiment 2*), we found that errors in joint coordinates exhibited consistent coupling such that errors were smaller for combinations of flexion or extension at both joints and larger for combinations flexion at one joint and extension at the other joint. Critically, this coupling of errors was similar to the coupling of errors predicted by the MB Model. This similarity between the predicted and actual coupling of errors highlights how biarticulars influence perceptual estimates of limb position.

METHODS

Musculoskeletal Models

We used two variants of the musculoskeletal model developed by Scott and Loeb (10) to explore the influence of biarticulars on estimates of limb position (see original paper for full details of the model. See online supplement for model code: https://doi.org/10.6084/m9.figshare.13501956.v1).

The first variant, monoarticular only (MO) model, produced errors expected for a two-joint limb with only monoarticulars (Fig. 1*A*). The second variant, monoarticular and biarticular (MB) model, produced errors expected for a two-joint limb with both monoarticulars and biarticulars (Fig. 1*B*).

For monoarticulars, changes in firing rates of individual muscle spindles (Δs) are related to changes in the angle of the spanned joint ($\Delta\Phi$), normalized by a scaling parameter (k) equal to the muscle's fascicle length divided by its moment arm:

$$\Delta s = \Delta\phi / k. \tag{1}$$

For biarticulars, changes in firing rates of individual muscle spindles are related to changes in the angle of either spanned joint. In the upper limb, for example, changes in firing rates of individual spindles (Δs) are related to changes in the angle of the shoulder ($\Delta\Phi_S$) or elbow ($\Delta\Phi_E$), normalized by their respective scaling parameters at the shoulder (k_S) and elbow (k_E):

$$\Delta s = (\Delta\phi_S / k_S) + (\phi_E / k_E). \tag{2}$$

The nervous system needs to perform the inverse operation to estimate limb position from firing rates of muscle spindles. If using information from only monoarticulars (MO model), errors in estimating the angles of the shoulder ($\Delta\Phi_S$) and elbow ($\Delta\Phi_E$) are proportional to the variability of firing rates of all spindles in the shoulder (ΔS_{SM}) and elbow (ΔS_{EM}) monoarticulars. Estimation errors are also influenced by scaling parameters equal to the mean fascicle length divided by the mean moment arm of the shoulder (k_{SM}) and elbow (k_{EM}) monoarticulars. The resulting estimates of angular errors at the shoulder and elbow can be expressed as follows:

$$\Delta\phi_S = k_{SM}\Delta S_{SM}, \tag{3}$$

$$\Delta\phi_E = k_{EM}\Delta S_{EM}. \tag{4}$$

If using information from both monoarticulars and biarticulars (MB model), errors in estimating the angles of the shoulder ($\Delta\Phi_S$) and elbow ($\Delta\Phi_E$) are proportional to the variability of firing rates of all spindles in the shoulder monoarticulars (ΔS_{SM}) and biarticulars (ΔS_{SB}) and elbow monoarticulars (ΔS_{EM}) and biarticulars (ΔS_{EB}). These estimation errors are also influenced by scaling parameters equal to the mean fascicle length divided by the mean moment arm of the shoulder monoarticulars (k_{SM}) and biarticulars (k_{SB}) and elbow monoarticulars (k_{EM}) and biarticulars (k_{EB}). Furthermore, errors in estimating shoulder angle are modulated by weighting factors proportional to the number of spindles in the shoulder monoarticulars (w_{SM}) and biarticulars (w_{SB}), where $w_{SM} + w_{SB} = 1$. Finally, errors in estimating elbow angle are modulated by weighting factors proportional to the number of spindles in the elbow monoarticulars (w_{EM}) and biarticulars (w_{EB}), where $w_{EM} + w_{EB} = 1$. The resulting estimates of angular errors at the shoulder ($\Delta\Phi_S$) and elbow ($\Delta\Phi_E$) can be expressed as follows:

$$\Delta\phi_S = w_{SM}k_{SM}\Delta S_{SM} + w_{SB}\left(k_{SB}\Delta S_{SB} - \frac{\Delta\phi_E k_{SB}}{k_{EB}}\right), \tag{5}$$

$$\Delta\phi_E = w_{EM}k_{EM}\Delta S_{EM} + w_{EB}\left(k_{EB}\Delta S_{EB} - \frac{\Delta\phi_S k_{EB}}{k_{SB}}\right). \tag{6}$$

The MO and MB models can also be combined with segment lengths of the upper-arm (L1, shoulder to elbow) and forearm (L2, elbow to fingertip) to estimate hand position in Cartesian coordinates (x, y):

$$x = L_1 cos(\phi_S^* + \Delta\phi_S) + L_2 cos(\phi_S^* + \Delta\phi_S + \phi_E^* + \Delta\phi_E), \tag{7}$$

$$y = L_1 sin(\phi_S^* + \Delta\phi_S) + L_2 cos(\phi_S^* + \Delta\phi_S + \phi_E^* + \Delta\phi_E). \tag{8}$$

Model Parameters

Table 1 specifies the values of the parameters used to simulate errors produced by both models. We assumed individual spindles produce errors that are independently drawn from a Gaussian distribution with a standard deviation of 0.5 radians (13) and muscle groups transmit errors equal to the average error produced by all individual spindles in each muscle group. Based on these assumptions, we simulated errors produced by a shoulder monoarticular group (ΔS_{SM}), shoulder biarticular group (ΔS_{SB}), elbow monoarticular group (ΔS_{EM}), and elbow biarticular group (ΔS_{EB}) by drawing errors for each group from a Gaussian distribution with a standard deviation of 0.5 and normalizing the error by the square root of the number of spindles in each muscle group

Table 1. *Values of parameters used for simulations of both models in experiments 1 and 2*

Muscle Group	Spindle Count	*k* Coefficient	Fascicle Length, cm	Moment Arm, cm
Shoulder Monoarticulars	549	4.7		
Pectoralis Major		3.4	13.7	4.0
Anterior Deltoid		5.8	9.9	1.7
Posterior Deltoid		4.8	12.0	−2.5
Supraspinatus		5.3	7.4	−1.4
Infraspinatus		4.1	7.8	−1.9
Shoulder Biarticulars	542	4.9		
Biceps Long Head		4.0	11.6	2.9
Biceps Short Head		5.2	15.0	2.9
Triceps Long Head		5.4	13.4	−2.5
Elbow Monoarticulars	785	4.6		
Brachioradialis		3.9	16.4	4.2
Brachialis		4.3	9.0	2.1
Triceps Lateral Head		5.7	11.4	−2.0
Triceps Medial Head		4.6	9.2	−2.0
Elbow Biarticulars	542	4.8		
Biceps Long Head		3.4	11.6	3.4
Biceps Short Head		4.4	15.0	3.4
Triceps Long Head		6.7	13.4	−2.0

(14). Spindle counts for the shoulder monoarticular group (n = 549), elbow monoarticular group (n = 785), and biarticular groups (n = 542) were based on spindle counts obtained from morphological studies of human muscles (6). Scaling parameters of each group (k_{SM} = 4.7, k_{SB} = 4.9, k_{EM} = 4.6, k_{EB} = 4.8) were computed from mean fascicle lengths and mean moment arms obtained from studies of human fascicle lengths (15–19) and moment arms (18–20). In both experiments, we computed errors in Cartesian hand coordinates using the actual segment lengths (L1 and L2) of each human subject. Finally, we performed sensitivity analyses that examined how model behavior was altered by 2 times, 4 times, and 8 times increases in the spindle counts of shoulder monoarticulars, elbow monoarticulars, and biarticulars.

Subjects

In *experiment 1*, we examined position sense in a cohort of 100 human subjects (61 female, 39 male) who had previously participated in a series of clinical studies in our laboratories (21–23). All subjects were right-handed and ranged in age from 20 to 65 yr (median = 44). All subjects had no history of neurological or orthopedic problems affecting either arm and provided informed consent before participation. Data were collected at Queen's University, St. Mary's of the Lake Hospital (both in Kingston, Ontario, Canada), and Foothills Hospital (Calgary, Alberta, Canada) as part of a standardized protocol.

In *experiment 2*, we examined position sense in eight, right-handed human subjects (4 female, 4 male) ranging in age from 20 to 27 yr (median = 23). All subjects had no history of neurological or orthopedic problems affecting either arm and provided informed consent before participation. Data were collected at New York Institute of Technology, College of Osteopathic Medicine (Old Westbury, New York).

Apparatus and Task

Data at all sites were collected using a Kinarm exoskeleton robot (24) (Kinarm Ltd., Kingston, Ontario). Subjects sat in a wheelchair base with each arm placed in an exoskeleton adjusted to the dimensions of their body. The robot supported the subjects' arms in the horizontal plane, monitored shoulder and elbow rotations, and could apply mechanical torques at the shoulder and/or elbow. Subjects could not view any part of their arms and hands, which were occluded from view by a metal partition and opaque fabric cover.

Limb position sense was quantified using an arm position matching task (21–23). Subjects were instructed to relax one arm and allow the robot to passively move it to different target positions within the horizontal plane. Passive movements followed linear paths with bell-shaped speed profiles (max speed $<$ 1 m/s). Subjects were further instructed to wait for the robot to stop moving their arm, then match the position by actively moving their opposite arm to the mirror location. The final hand position at the end of each trial was used as the start position for the next trial.

Subjects were given as much time as they wanted and were allowed to make as many corrective movements as they wanted to complete each trial. They verbally indicated when they completed each trial to the examiner, who then manually triggered the next trial. On average, subjects took 2.41 ± 0.85 s to complete each trial in *experiment 1* and 2.65 ± 0.48 s to complete each trial in *experiment 2*.

In *experiment 1*, the passive arm was randomly moved to nine different target positions organized in a 3 × 3 grid in Cartesian hand coordinates (Fig. 2*A*). The central target was located at the position of each subject's index fingertip when their shoulder was in 30° of forward flexion and their elbow was in 90° of flexion. This position defined the origin in hand coordinates (0 cm, 0 cm), and the other eight targets were distributed in a 20 cm by 20 cm square around the central target: (10 cm, 0 cm), (10 cm, 10 cm), (0 cm, 10 cm), (−10 cm, 10 cm), (−10 cm, 0 cm), (−10 cm, −10 cm), (0 cm, −10 cm), and (10 cm, −10 cm). However, due to individual differences in upper-arm (L1) and forearm (L2) lengths, the central target of each subject was located at a different position in hand coordinates, resulting in a mean position of 1.5 cm

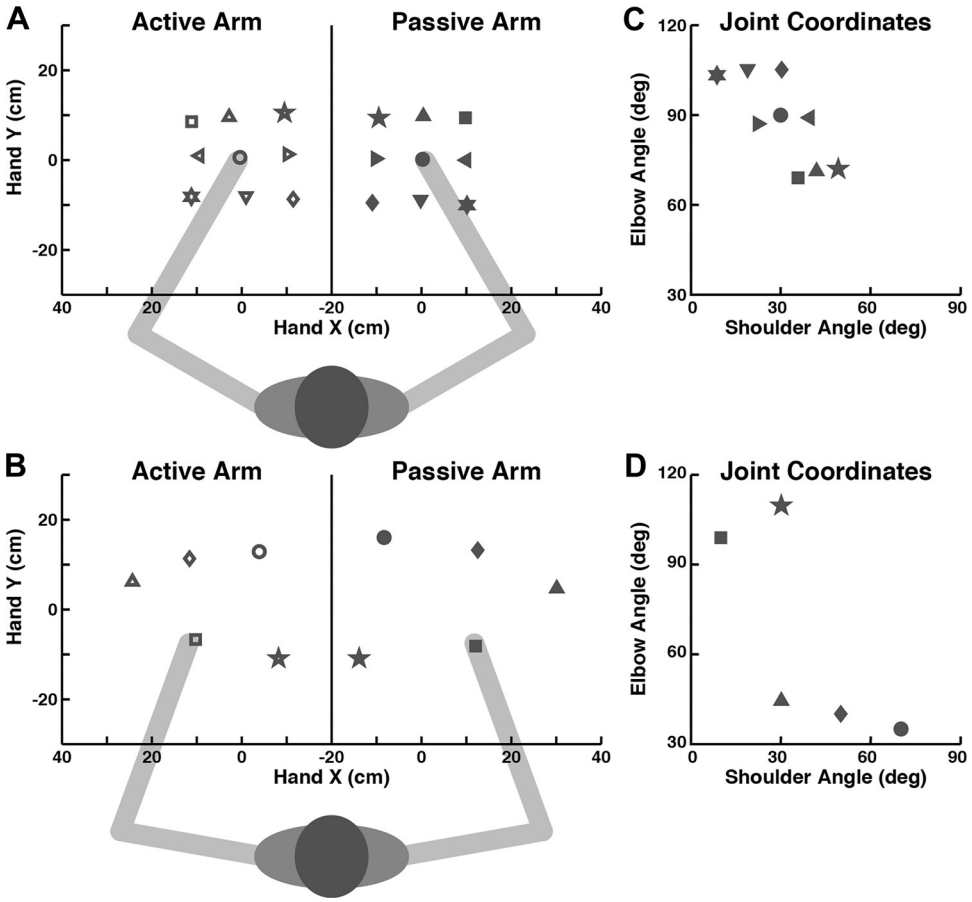

Figure 2. Task designs used in *experiment 1* (*A* and *C*) and *experiment 2* (*B* and *D*). *A* and *B*: average target positions of the passive arm (filled symbols) and average matching positions of the active arm (open symbols) from two exemplar subjects in hand coordinates (*x, y*). *C* and *D*: average angles of the passive arm (filled symbols) from the same subjects in joint coordinates (*shoulder, elbow*). In *experiment 1*, either the right or left hand was passively moved to one of nine target locations specified in hand coordinates: (0 cm, 0 cm), (10 cm, 0 cm), (10 cm, 10 cm), (0 cm, 10 cm), (−10 cm, 10 cm), (−10 cm, 0 cm), (−10 cm, −10 cm), (0 cm, −10 cm), (10 cm, −10 cm). In *experiment 2*, the right hand was moved to one of five target locations specified in joint coordinates: (30°, 110°), (5°, 100°), (30°, 45°), (50°, 40°), (70°, 35°).

lateral and 49.2 cm distal from the shoulder. In addition, although the joint angles (*shoulder, elbow*) of the central target were fixed at (30°, 90°), the angles of the eight peripheral targets varied between subjects, resulting in mean angles (22°, 88°), (41°, 59°), (49°, 62°), (59°, 61°), (44°, 87°), (30°, 109°), (15°, 110°), and (3°, 107°) in joint coordinates (Fig. 2*C*). Each subject completed six trials to each of the nine target positions for a total of 54 trials. After completing one block using one arm (selected randomly), subjects completed a second block using the opposite arm.

In *experiment 2*, we used a similar protocol with three key exceptions (Fig. 2*B*). First, we employed five targets that were specified in joint (*shoulder, elbow*) coordinates: (30°,110°), (5°, 100°), (30°, 45°), (50°, 40°), and (70°, 35°). This allowed us to assess larger ranges of shoulder and elbow angles than in *experiment 1* (Fig. 2, *C* and *D*). However, because the five targets were specified in joint coordinates, their positions in hand coordinates varied between subjects. On average, the origin in hand coordinates (0 cm, 0 cm) was located 3.1 cm lateral and 51.0 cm distal from the shoulder, and the five targets were located at (13 cm, −8 cm), (31 cm, 5 cm), (−13 cm, −11 cm), (13 cm, 14 cm), and (−7 cm, 16 cm) relative to the origin. Accordingly, this also allowed us to assess a larger range of hand positions than in *experiment 1* (Fig. 2, *A* and *B*). Second, all subjects performed 150 trials to each target position (25 times more than *experiment 1*). This allowed us to assess individual patterns of errors in estimating arm position at each target. Due to the length of this experiment (750 trials total), subjects performed three blocks of 250 trials composed of 50 trials to each target position and were given rest breaks after each block. Third, subjects performed all 750 trials using only their right arm as the passive arm and their left arm as the active arm.

Data Analyses

We investigated the influence of biarticulars on errors in estimating arm position by examining two-dimensional distributions of errors in Cartesian hand (*x, y*) and joint (*shoulder, elbow*) coordinates. We analyzed errors in hand coordinates to facilitate comparisons between our study and previous studies of end point errors in hand coordinates (25–30). We analyzed errors in joint coordinates because the nonlinear mapping between hand and joint coordinates creates a clear dissociation between the distributions of errors predicted by the MO and MB models in joint coordinates (Fig. 1*D*).

Errors predicted by the MO and MB models in hand and joint coordinates were simulated by running each model through the same number of trials (iterations) that our human subjects completed to each of the nine targets in *experiment 1* (n = 1,200: 100 subjects × 2 arms × 6 trials per target) and each of the five targets in *experiment 2* (n = 1,200: 8 subjects × 150 trials per target). Shoulder and elbow errors predicted by the MO model in both experiments were obtained from *Eqs. 3* and *4*. Shoulder and elbow errors predicted by the MB model in both experiments were obtained

from *Eqs. 5* and *6*. Predicted errors in hand coordinates were obtained from *Eqs. 7* and *8*, using the shoulder and elbow errors from each model and actual segment lengths (L1 and L2) of each human subject in *experiments 1* and *2* as inputs.

Errors made by our human subjects in hand and joint coordinates were compared with the predicted errors from the two models. Errors in hand coordinates were obtained from the medial-lateral (x) and proximal-distal (y) positions of each index fingertip relative to the origin (0 cm, 0 cm) when the shoulder was in 30° of forward flexion and the elbow was in 90° of flexion. In both experiments, errors were initially calculated by subtracting the actual fingertip positions and joint angles of the passive arm at the end of each trial from the actual fingertip positions and joint angles of the active arm at the end of each trial. By subtracting the actual, rather than the desired, fingertip positions and joint angles of the passive arm, we removed any small differences between the actual and desired positions and angles of the passive arm from each hand and joint error. In both experiments, we then subtracted each subject's mean hand and joint errors at each target from their hand and joint errors on each trial. This step removed all systematic biases from each subject's hand and joint errors (21–23). In *experiment 1*, we finally grouped all hand and joint errors for each of the nine targets (1,200 trails/target: 100 subjects × 2 arms × 6 trials). In *experiment 2*, we grouped each subject's hand and joint errors for each block of 50 trials to each target and removed any potential drifts in proprioception (31–33) by using linear regression to subtract the running mean from each block of 50 trials to each target (Supplemental Fig. S1; https://doi.org/10.6084/m9.figshare.12552140.v1). We finally grouped all hand and joint errors made by each subject to each of the five targets (150 trials/group, 40 groups: 8 subjects × 5 targets) in *experiment 2*.

We analyzed two measures obtained from principle components analyses (PCA) performed on the distributions of errors from the musculoskeletal models and human subjects for each target in *experiment 1* and for each target per subject in *experiment 2*. The "axis" (υ) describes the eigenvector (angle) of the major PCA component, where ω_1 and ω_2 are the weights for the eigenvector of the major PCA component. The "elongation" (ε) describes the anisotropy of the major and minor PCA components, where λ_1 and λ_2 are the eigenvalues (variances) of the major and minor PCA components:

$$\upsilon = tan^{-1}\left(\frac{\omega_2}{\omega_1}\right), \tag{9}$$

$$\varepsilon = \sqrt{\frac{(\lambda_1 - \lambda_2)^2}{(\lambda_1{}^2 + \lambda_2{}^2)}}. \tag{10}$$

In *experiment 1*, we used the grouped data from each of the nine targets to compute nine summary measures of Axes and Elongation for the MO model, MB model, and human subjects. In *experiment 2*, we used the data from each of the 40 groups (8 subjects × 5 targets) to compute 40 summary measures of axis and elongation for the MO model, MB model, and human subjects. First, we analyzed differences between the predictions made by the two models in each experiment. We used Watson–Williams tests to compare the mean axis of the two models in hand and joint coordinates and Wilcoxon rank-sum tests to compare the mean elongation of the two models in hand and joint coordinates for a total of four tests in each experiment. The threshold for significance in each experiment was set at $P < 0.0125$ using a Bonferroni correction (α/n), where $\alpha = 0.05$ and $n = 4$ tests in each experiment. Second, we analyzed differences between the actual performance of our human subjects and the predictions made by the two models in each experiment. We used Watson–Williams tests to compare the mean axis of the human subjects with each model in hand and joint coordinates and Wilcoxon rank-sum tests to compare the mean elongation of human subjects with each model in hand and joint coordinates, for a total of eight tests in each experiment. The threshold for significance in each experiment was set at $P < 0.00625$ using a Bonferroni correction (α/n), where $\alpha = 0.05$ and $n = 8$ tests in each experiment.

RESULTS

Experiment 1: Distributions of Errors in Hand Coordinates

In hand coordinates, both the monoarticular only (MO) and the monoarticular and biarticular (MB) models produced elliptical distributions of errors that featured greater medial-lateral than proximal-distal variability (Fig. 3, *A* and *B*). The MO model had a mean axis of 5.3° and mean elongation of 0.92, and the MB model had a mean axis of −2.8° and mean elongation 0.71 (Table 2, Fig. 3*D*). We did not find a significant difference between the mean axis of the two models ($P = 0.11$), but we observed a significant difference between their mean elongation ($P < 0.0125$). In agreement with our hypothesis (Fig. 1*E*), this shows that the biarticular group reduced the medial-lateral variability of position sense in hand coordinates.

The grouped data from our human subjects also produced elliptical distributions of errors in hand coordinates that featured greater medial-lateral than proximal-distal variability (Fig. 3*C*). The distributions of errors had a mean axis of 1.1° and mean elongation of 0.73 (Table 2, Fig. 3*D*). Their mean axis was not significantly different than in the MO model ($P = 0.16$) or MB model ($P = 0.40$), nor was their mean elongation significantly different than in the MB model ($P = 0.93$). However, their mean elongation was significantly different than in the MO model ($P < 0.00625$), indicating that the MO model did not accurately predict the variability of position sense of our human subjects in hand coordinates.

Experiment 1: Distributions of Errors in Joint Coordinates

As expected, the MO model produced circular distributions of errors in joint coordinates (Fig. 4*A*), whereas the MB model produced elliptical distributions of errors that coupled flexion errors at one joint with extension errors at the other joint (Fig. 4*B*). The MO model had a mean axis of 1.2° and mean elongation of 0.35, whereas the MB model had a mean axis of −38.8° and mean elongation 0.74 (Table 2, Fig. 4*D*). Importantly, the models exhibited significant differences in both their mean axis ($P < 0.0125$) and mean elongation ($P < 0.0125$). In agreement with our hypothesis (Fig.

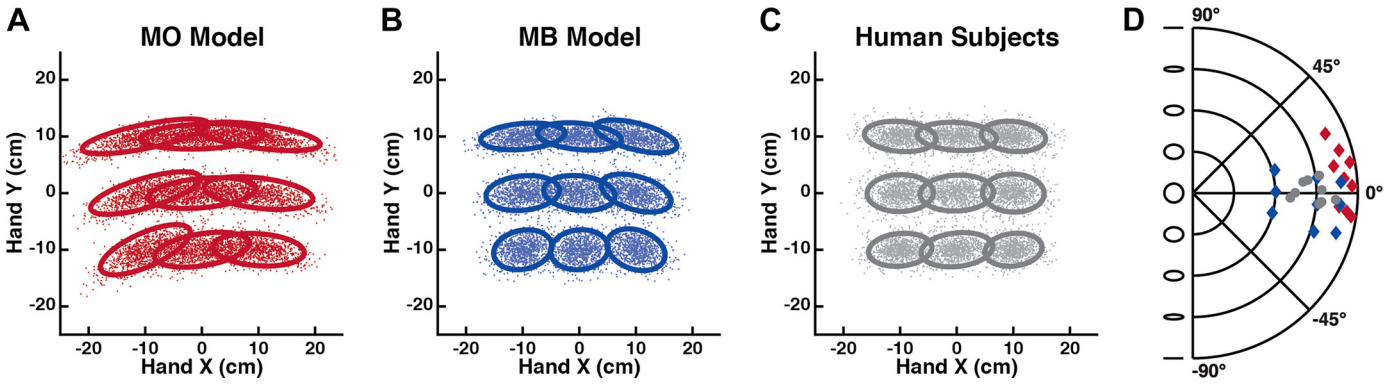

Figure 3. *Experiment 1*: model predictions and human data in hand coordinates. *A*–*C*: distributions of errors from the monoarticular only (MO) model, monoarticular and biarticular (MB) model, and human subjects (all subjects and arms grouped) to each of the nine targets in Cartesian, hand (*x*, *y*) coordinates. Dots show errors on individual trials to each target and ellipses illustrate principle components analyses (PCA) ellipses fit to the distributions of errors at each target. Dots and ellipses are plotted relative to specified location of each target in hand (*x*, *y*) coordinates: (0 cm, 0 cm), (10 cm, 0 cm), (10 cm, 10 cm), (0 cm, 10 cm), (−10 cm, 10 cm), (−10 cm, 0 cm), (−10 cm, −10 cm), (0 cm, −10 cm), and (10 cm, −10 cm). *D*: polar plots showing the axes (angle) and elongation (magnitude) associated with the distributions of errors from the MO model (red diamonds), MB model (blue diamonds), and human subjects (gray circles) to each of the nine targets in hand coordinates.

1*D*), this shows that the biarticular group altered the predicted orientation and shape of position sense variability in joint coordinates.

Similar to the MB model, the grouped data of our human subjects produced elliptical distributions of errors that coupled flexion errors at one joint with extension errors at the other joint (Fig. 4*C*). The distributions of errors had a mean axis of −40.6° and mean elongation of 0.68 (Table 2, Fig. 4*D*), which were not significantly different than the mean axis ($P = 0.17$) and mean elongation ($P = 0.09$) of the MB model. However, they were significantly different than the mean axis ($P < 0.00625$) and mean elongation ($P < 0.00625$) of the MO model, indicating that the MO model did not accurately predict the variability of position sense of our human subjects in joint coordinates.

We subsequently examined how the distributions of errors predicted by the MO and MB models in joint coordinates were influenced by altering the spindle counts, fascicle lengths, or moment arms of the shoulder monoarticular group (Supplemental Fig. S2; https://doi.org/10.6084/m9.figshare.12552176.v1), elbow monoarticular group (Supplemental Fig. S3; https://doi.org/10.6084/m9.figshare.12552182.v1) or biarticular group (Supplemental Fig. S4; https://doi.org/10.6084/m9.figshare.12552188.v1). After altering the shoulder monoarticulars by increasing the spindle count, decreasing the mean fascicle length, or increasing the mean moment arm, the MO model produced distributions of errors with greater elongation along the elbow axis (Supplemental Fig. S2, *A*–*C*). In contrast, the MB model produced distributions of errors that exhibited increases in elongation coupled with rotation toward the elbow axis (Supplemental Fig. S2, *D*–*F*). When the elbow monoarticular group was modified, the MO model produced distributions of errors with greater elongation along the shoulder axis (Supplemental Fig. S3, *A*–*C*), whereas the MB model exhibited increases in elongation coupled with rotation toward the shoulder axis (Supplemental Fig. S3, *D*–*F*). Finally, modifying the biarticulars could not affect the MO model (not illustrated), but the distributions of errors produced by the MB model exhibited increases in elongation without any rotation (Supplemental Fig. S4, *A*–*C*). Importantly, regardless of the model parameters, the MO model never produced elliptical distributions of errors that coupled flexion errors or extension errors at both joints.

Given the broad age range of our subjects in *experiment 1*, we also examined the effects of aging on errors estimating arm position (Supplemental Fig. S5; https://doi.org/10.6084/m9.figshare.12552191.v1). In this analysis, we compared subjects in the bottom age quartile (young group: age ≤ 30 yr) with subjects in the top age quartile (older group: age ≥ 55 yr). Based on the results of our previous study on the effects of aging on position sense (22), we expected to observe higher variability in estimates of arm position (measured as the area of PCA ellipses) in the older group, but we did not expect to observe differences in the mean axis or mean elongation of the two groups. As expected, we found that the variability of errors in joint coordinates was significantly higher

Table 2. *Results of the musculoskeletal models and human subjects in experiments 1 and 2*

		Experiment 1			*Experiment 2*		
Coordinate	**Measure**	**MO Model**	**MB Model**	**Subjects**	**MO Model**	**MB Model**	**Subjects**
Hand	Axis	5.3° (11.2°)	−2.8° (9.2°)	1.1° (4.4°)	−4.7° (17.6°)	−10.7° (17.6°)	−7.9° (15.0°)
	Elongation	**0.92 (0.04)**	0.71 (0.18)	0.73 (0.08)	**0.94 (0.05)**	0.80 (0.20)	0.83 (0.12)
Joint	Axis	**1.2° (3.2°)**	−38.8° (1.3°)	−40.6° (8.8°)	**−1.0° (8.0°)**	−38.4° (2.7°)	−41.5° (16.3°)
	Elongation	**0.35 (0.05)**	0.74 (0.02)	0.68 (0.08)	**0.36 (0.09)**	0.75 (0.03)	0.74 (0.17)

Values for each measure show the means (SD). Boldface values show measures in which the model is significantly different than the other model ($P < 0.0125$) and significantly different than the human subjects ($P < 0.00625$).

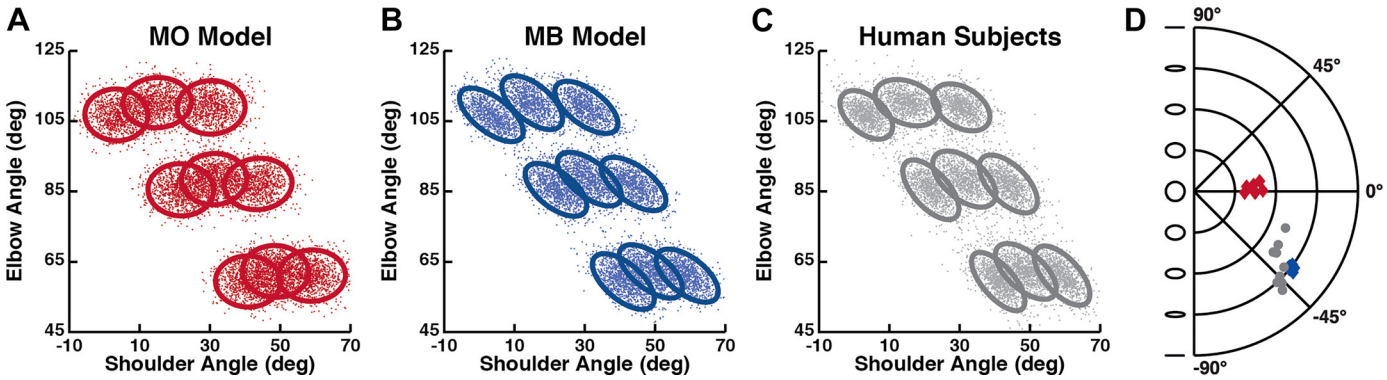

Figure 4. Model predictions and human data from *experiment 1* in joint coordinates. *A*–*C*: distributions of errors from the monoarticular only (MO) model, monoarticular and biarticular (MB) model, and human subjects (all subjects and arms grouped) to each of the nine targets in Cartesian, joint (*shoulder, elbow*) coordinates. Dots show errors on individual trials to each target and ellipses illustrate principle components analyses (PCA) ellipses fit to the distributions of errors to each target. Dots and ellipses are plotted relative to the average location of each target in joint (*shoulder, elbow*) coordinates: (30°, 90°), (22°, 88°), (41°, 59°), (49°, 62°), (59°, 61°), (44°, 87°), (30°, 109°), (15°, 110°), and (3°, 107°). *D*: polar plots showing the axes (angle) and Elongation (magnitude) associated with the distributions of errors from the MO model (red diamonds), MB model (blue diamonds), and human subjects (black circles) to each of the nine targets in joint coordinates.

in the older group ($P < 0.001$). Furthermore, the mean axis of both groups was not significantly different ($P = 0.42$). However, the mean elongation was significantly smaller (more circular) in the older group ($P = 0.002$).

Experiment 2: Distributions of Errors in Hand Coordinates

Although *experiment 2* examined a broader range of hand positions, both models displayed similar results to *experiment 1* in hand coordinates. Notably, both models produced elliptical distributions of errors with greater medial-lateral than proximal-distal variability (Fig. 5, *A* and *B*). The MO model had a mean axis of −4.7°and a mean elongation of 0.94, whereas the MB model had a mean axis of −10.6° and a mean elongation of 0.80 (Table 2, Fig. 5*D*). We did not find a significant difference between the mean axis of the two models ($P = 0.14$), but we did observe a significant difference between their mean elongations ($P < 0.0125$). In agreement with our hypothesis (Fig. 1*E*), this shows that the biarticular group reduced the medial-lateral variability of position sense in hand coordinates.

Similar to both models, the exemplar subject illustrated in Fig. 5*C* produced elliptical distributions of errors with greater medial-lateral than proximal-distal variability. The grouped data ($n = 40$, 8 subjects × 5 targets) had a mean axis of −7.9° and a mean elongation of 0.83 (Table 2, Fig. 5*D*). The mean axis was not significantly different than in the MO model ($P = 0.44$) or MB model ($P = 0.39$), nor was the mean elongation significantly different than the MB model ($P = 0.19$). However, the mean elongation was significantly different than in the MO model ($P < 0.00625$). Similar to *experiment 1*, this also indicates that the MO model did not accurately predict the variability of position sense of our human subjects in hand coordinates.

Experiment 2: Distributions of Errors in Joint Coordinates

Although we examined a broader range of shoulder and elbow angles in *experiment 2*, both models produced similar

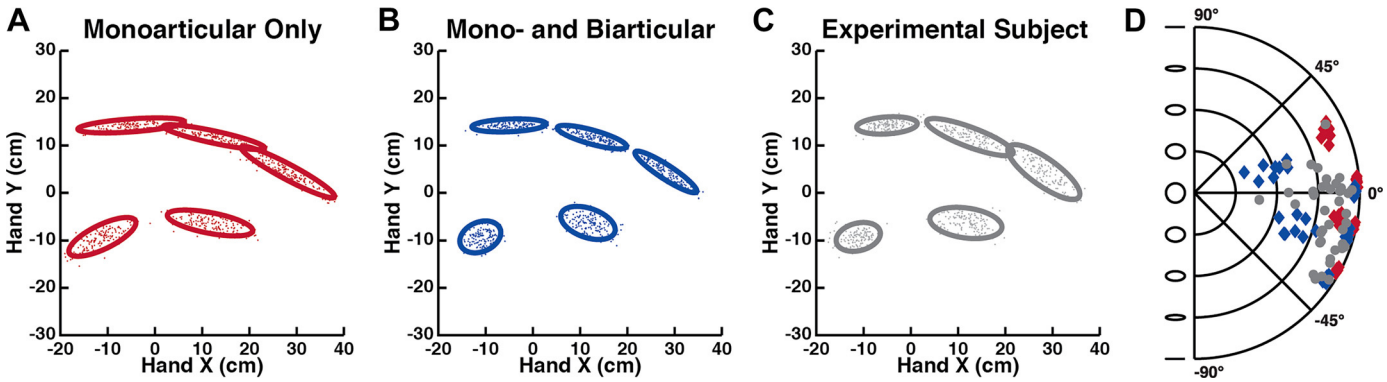

Figure 5. *Experiment 2*: model predictions and human data in hand coordinates. *A*–*C*: distributions of errors from the monoarticular only (MO) model, monoarticular and biarticular (MB) model, and an exemplar human subject to each of the five targets in Cartesian, hand (*x, y*) coordinates. Dots show errors on individual trials to each target and ellipses illustrate principle components analyses (PCA) ellipses fit to the distributions of errors to each target. Dots and ellipses are plotted relative to the average location of each target in hand (*x, y*) coordinates: (13 cm, −8 cm), (31 cm, 5 cm), (−13 cm, −11 cm), (13 cm, 14 cm), and (−7 cm, 16 cm). *D*: polar plots showing the axes (angle) and elongation (magnitude) associated with the distributions of errors from the MO model (red diamonds), MB model (blue diamonds), and human subjects (gray circles) to each of the 40 groups (8 subjects × 5 targets) in hand coordinates.

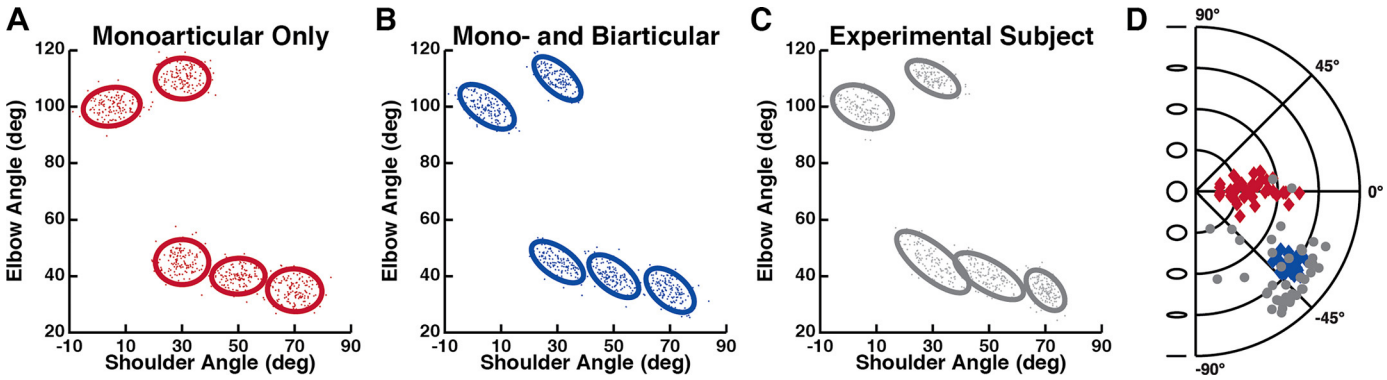

Figure 6. *Experiment 2*: model predictions and human data in joint coordinates. *A–C*: distributions of errors from the monoarticular only (MO) model, monoarticular and biarticular (MB) model, and an exemplar human subject to each of the five targets in Cartesian, joint (*shoulder, elbow*) coordinates. Dots show errors on individual trials to each target and ellipses illustrate principle components analyses (PCA) ellipses fit to the distributions of errors to each target. Dots and ellipses are plotted relative to the specified location of each target in joint (*shoulder, elbow*) coordinates: (30°, 110°), (5°, 100°), (30°, 45°), (50°, 40°), and (70°, 35°). *D*: polar plots showing the axes (angle) and elongation (magnitude) associated with the distributions of errors from the MO model (red diamonds), MB model (blue diamonds), and human subjects (black circles) to each of the 40 targets (8 subjects × 5 targets) in joint coordinates.

results to *experiment 1* in joint coordinates. Notably, the MO model produced circular distributions of errors (Fig. 6*A*) with a mean axis of −0.1° and mean elongation of 0.36 (Table 2, Fig. 6*D*). In contrast, the MB model produced elliptical distributions that coupled flexion errors at one joint with extension errors at the other joint (Fig. 6*B*), resulting in a mean axis of −38.4° and mean elongation of 0.75 (Table 2, Fig. 6*D*). Importantly, the MO and MB models exhibited significant differences between their mean axis ($P < 0.0125$) and mean elongation ($P < 0.0125$). In agreement with our hypothesis (Fig. 1*D*), this demonstrates the predicted orientation and shape of position sense variability in joint coordinates was altered by the biarticular group.

Similar to the grouped data in *experiment 1*, the exemplar subject illustrated in Fig. 6*C* exhibited elliptical distributions of errors that coupled flexion errors at one joint with extension errors at the other joint. The grouped data (n = 40: 5 targets × 8 subjects) had a mean axis of −41.5° and mean elongation of 0.74 (Table 2, Fig. 6*D*), which were not significantly different than the mean axis (P = 0.15) and mean elongation (P = 0.07) of the MB model. However, they were significantly different than the mean axis ($P < 0.00625$) and mean elongation ($P < 0.00625$) of the MO model. In agreement with *experiment 1*, this also indicates that the MO model did not accurately predict the variability of position sense of our human subjects in joint coordinates.

We subsequently examined how the distributions of errors predicted by the MO and MB models in joint coordinates were influenced by modifying the spindle counts, fascicle lengths, or moment arms of the shoulder monoarticular group (Supplemental Fig. S6; https://doi.org/10.6084/m9.figshare.12552194.v1), elbow monoarticular group (Supplemental Fig. S7; https://doi.org/10.6084/m9.figshare.12552200.v1), or biarticular group (Supplemental Fig. S8; https://doi.org/10.6084/m9.figshare.12552215.v1). Notably, altering the model parameters in *experiment 2* produced results that were similar to those in *experiment 1*. When the shoulder or elbow monoarticulars were altered by increasing the spindle count, decreasing the mean fascicle length or increasing the mean moment arm, the MO model produced distributions of errors with greater elongation along the elbow axis (Supplemental Fig. S6, *A–C*) or shoulder axis (Supplemental Fig. S7, *A–C*). In contrast, the distributions of errors produced by the MB model exhibited increases in elongation coupled with rotation toward the elbow (Supplemental Fig. S6, *D–F*) or shoulder (Supplemental Fig. S7, *D–F*) axis. Finally, when the biarticulars were modified, the distributions of errors produced by the MB model exhibited increases in elongation without associated rotations (Supplemental Fig. S8, *A–C*). Importantly, the MO model did not produce elliptical distributions of errors that coupled flexion errors or extension errors at both joints as a result of any of the modifications to the different muscle groups.

DISCUSSION

The present study examined the influence of biarticulars on perceptual estimates of limb position. We compared simulated distributions of errors obtained from two musculoskeletal models with actual distributions of errors obtained from human subjects. Novel to this study, we examined the role of biarticulars by comparing predictions from a model with monoarticulars only (MO model) with a model that included both monoarticulars and biarticulars (MB model). Unlike previous studies, which mainly focused on examining distributions of errors in hand coordinates, we also examined distributions of errors in joint coordinates. Notably, our musculoskeletal models predicted some differences in hand coordinates but greater differences in joint coordinates. This does not provide evidence in favor of one particular coordinate system but highlights the benefits of using multiple views to examine predictions of nonlinear systems.

Our analysis in joint coordinates revealed that our two models predicted different distributions of errors in both experiments. The MO model predicted circular distributions of errors in joint coordinates, whereas the MB model predicted elliptical distributions of errors that would exhibit systematic coupling between flexion errors at one joint and extension errors at the other joint. Our population

(*experiment 1*) and individual subjects (*experiment 2*) also produced elliptical distributions of errors that exhibited systematic coupling between flexion errors at one joint and extension errors at the other joint. Critically, our human data qualitatively and quantitatively matched the distinctive patterns of errors produced by the MB model in joint coordinates. This provides clear evidence that sensory information from biarticulars influences our estimation of limb position throughout the arm's entire workspace.

Our findings are particularly important because few empirical studies have examined the influence of biarticulars on perception. As previously stated, we are only aware of one empirical study that examined the influence of biarticulars on proprioception (12). This study found that detection thresholds for passive wrist (elbow) rotation increased when the elbow (wrist) was concurrently rotated in the opposite direction. These opposing joint rotations would produce minimal changes in the length of the distal biarticulars because they cross the elbow and wrist on the same side. Similarly, we also observed larger errors during opposing rotations of the shoulder and elbow, which would lead to minimal changes in length of the proximal biarticulars because they cross the shoulder and elbow on the same side.

Two previous modeling studies have also investigated the influence of biarticulars on perceptual estimation. In the first study, Scott and Loeb (10) explored the optimal distributions of muscle spindles in shoulder monoarticulars, elbow monoarticulars, and elbow-shoulder biarticulars for encoding sensory information in three different coordinate frames. They found that the muscle spindles of biarticulars were important for encoding information in segment orientation and end point coordinates. However, they also demonstrated that the actual distribution of muscle spindles in humans is not ideally suited for encoding information in any particular coordinate frame. In the other study, Smeets (11) examined the influence of biarticulars on estimates of hand movement by comparing two models, one with only monoarticulars at the shoulder and elbow and one with monoarticulars at the shoulder and biarticulars at both joints. This study found that the model with biarticulars provided more uniform sensitivity to different directions of hand movement than the model with only monoarticulars. Our findings are similar in that the MB model predicted less elongated errors in hand coordinates than the MO model.

In contrast to the lack of research on the influence of biarticulars on perceptual estimates, several empirical and theoretical studies have examined the influence of biarticulars on motor control. In brief, biarticulars enable efficient transfer of energy across joints (34–37). They also create biased patterns of muscle activity (1, 6, 38) that are appropriate for minimizing overall effort (3, 5, 11, 39). Furthermore, primary motor cortex and red nucleus exhibit a parallel bias in which more neurons are maximally active when flexor torques at one joint are coupled with extensor torques at the other (2, 40, 41).

Although our study focused on the influence of muscle spindles in estimating limb position, sensory information from Golgi tendon organs (GTOs) and cutaneous receptors may also contribute to estimating limb position. GTOs directly measure tendon strain and are ideally suited to account for changes in tendon length with different load levels and help estimate the length of the muscle-tendon complex (42). This is important for providing a consistent relation between sensory signals from muscles and segmental variables like joint angle. In our study, we would expect GTOs in the arm that was passively moved by the robot to exhibit little activity because the arms were supported against gravity and small loads were used to passively move the arm. Even if muscles were required to counter gravity or other external loads, similar biases would be expected because GTOs are in series with the muscles. Specifically, flexion at one joint coupled with extension at the other joint would lead to minimal changes in muscle length sensed by the spindles or muscular force sensed by GTOs.

Previous studies have also shown that cutaneous receptors contribute to perception of joint angle. This influence is notable for the fingers (43, 44) as well as more proximal joints such as the knee and elbow (28, 45). However, muscle spindles located within muscles that cross proximal limb joints may make a greater contribution to perception of limb position. Notably, perception of hand motion is attenuated by anesthetizing the skin around the fingers (46–48), whereas perception of proximal limb motion is not attenuated by anesthetizing the skin around the knee (49). Furthermore, more muscle spindles are located within muscles that cross proximal limb joints (10), whereas the density of cutaneous receptors is much greater distally (50).

It is possible that the observed coupling between flexion errors at one joint and extension errors at the other joint was related to specifics of our task, given that distinct perceptual, cognitive, and motor demands of different tasks can influence estimates of limb position (51). For example, tasks that use active arm movements to match the previous position of the same arm require a working memory component (25, 30, 52–54). In contrast, tasks that use active movements of one arm to match the position of the opposite arm circumvent the working memory component but require transfer of proprioceptive information between the two cerebral hemispheres (26, 27, 29, 51, 52, 55). Although working memory and interhemispheric transfer can influence estimates of arm position (51), the effects of interhemispheric transfer are relatively small. Accordingly, it is unlikely that the interhemispheric transfer required by our task can account for the coupling in joint coordinates observed in our task.

Other tasks have used a visual pointer/target (27, 54, 56) or a forced-choice response (27, 57) to avoid the potential influence of active arm movements on estimates of arm position. However, these tasks are not feasible for measuring both the magnitude and direction of two-dimensional errors in hand and joint coordinates. Instead, we allowed our subjects to directly compare the positions of their arms for as long as necessary before indicating that they had finished estimating their arm position. This permitted our subjects to maximize their use of proprioceptive information and minimize any influences of their active movements on estimates of their arm position. Both arms were also supported against gravity to avoid any influences resulting from effort needed to stabilize the arms against gravity (58, 59). Furthermore, both arms were occluded from vision to prevent any influences related to multisensory integration of vision and proprioception (29).

Another worthwhile discussion point is the value of examining both hand and joint coordinates in the current study. Although considerable effort has been dedicated to the issue of coordinate frames [for reviews, see Soechting and Flanders (60) and Battaglia-Mayer et al. (61)], it is important to emphasize that we did not examine hand and joint coordinates to argue for or against a particular coordinate frame. In fact, muscle spindle distributions may not optimally encode information in any particular coordinate frame (10). We also agree that there may be limited value in analyzing different coordinate frames for the purpose of revealing what coordinate frames are used to encode information (62–65).

Our use of an active movement paradigm could conflate sensory errors with motor noise. However, we do not think this compromised our results as subjects did not have time constraints to complete their matching movements and, unlike typical reaching movements, their matching movements often took a long time to complete and included multiple submovements. Furthermore, reaching movements to external targets usually produce variability ellipses that are primarily oriented along the direction of movement (66, 67). In the task used in *experiment 1*, movements to the central target would have produced variability ellipses at different angles and that would have resulted in a net circular distribution. Our findings are not consistent with these predicted patterns, although a complete answer would require modeling how monoarticulars and biarticulars are coordinated to achieve a particular task goal and how end point errors are impacted by particular noise distributions. Although this would be a worthwhile aim, it is beyond the scope of this paper.

As mentioned previously, we analyzed errors in joint coordinates because of the clear dissociation between the distributions of errors predicted by the MO and MB models that is present in joint but not hand coordinates (Table 2). Our analysis of errors in joint coordinates was crucial for demonstrating that biarticulars influence estimates of arm position. In addition, we examined errors in hand coordinates to facilitate comparisons between the results of this study and previous studies using hand coordinates (25–30). Our analysis of errors in hand coordinates found that our musculoskeletal models and human subjects exhibited greater medial-lateral than proximal-distal variability in both experiments. This is broadly consistent with previous empirical studies of errors estimating arm position in hand coordinates (29, 30). It is also consistent with previous modeling studies that explored the influence of biarticular muscles on estimates of arm position and movement (10, 11). Importantly, the action of biarticulars tends to reduce this bias, thus improving perception of limb position in external space. Given that virtually all biarticulars of the upper and lower limbs couple either flexion or extension across both spanned joints (except sartorius), this anatomical pattern benefits our perception of hand and foot position relative to our body.

ACKNOWLEDGMENTS

We would like to thank H. Bretzke, A.M. Coderre, M.J. Demers, M. Metzler, K. Moore, J. Peterson, M. Piitz, and J. Yajure for their help with recruitment, data collection, and technical support.

GRANTS

The present research was supported by a Canadian Institutes of Health Research Operating Grant (MOP 81366) and a National Science and Engineering Research Council Strategic Grant (2451-06).

DISCLOSURES

S.H.S. is cofounder and Chief Scientific Officer of Kinarm, which commercializes the Kinarm robot used in the present study.

AUTHOR CONTRIBUTIONS

T.M.H., I.K., S.P.D., and S.H.S. conceived and designed research; T.M.H., I.K., L.G., F.C., and S.P.D. performed experiments; T.M.H. analyzed data; T.M.H., I.K., S.P.D., and S.H.S. interpreted results of experiments; T.M.H. prepared figures; T.M.H. drafted manuscript; T.M.H., I.K., S.P.D., and S.H.S. edited and revised manuscript; T.M.H., I.K., and S.H.S. approved final version of manuscript.

ENDNOTE

At the request of the authors, readers are herein alerted to the fact that additional materials related to this manuscript may be found at https://doi.org/10.6084/m9.figshare.13501956.v1. These materials are not a part of this manuscript, and have not undergone peer review by the American Physiological Society (APS). APS and the journal editors take no responsibility for these materials, for the website address, or for any links to or from it.

REFERENCES

1. **Buchanan TS**, **Rovai GP**, **Rymer WZ.** Strategies for muscle activation during isometric torque generation at the human elbow. *J Neurophysiol* 62: 1201–1212, 1989. doi:10.1152/jn.1989.62.6.1201.
2. **Herter TM**, **Takei T**, **Munoz DP**, **Scott SH.** Neurons in red nucleus and primary motor cortex exhibit similar responses to mechanical perturbations applied to the upper-limb during posture. *Front Integr Neurosci* 9: 29, 2015. doi:10.3389/fnint.2015.00029.
3. **Kurtzer I**, **Pruszynski JA**, **Herter TM**, **Scott SH.** Primate upper limb muscles exhibit activity patterns that differ from their anatomical action during a postural task. *J Neurophysiol* 95: 493–504, 2006. doi:10.1152/jn.00706.2005.
4. **Kurtzer I**, **Herter TM**, **Scott SH.** Non-uniform distribution of reach-related and torque-related activity in upper arm muscles and neurons of primary motor cortex. *J Neurophysiol* 96: 3220–3230, 2006. doi:10.1152/jn.00110.2006.
5. **Nozaki D**, **Nakazawa K**, **Akai M.** Muscle activity determined by cosine tuning with a nontrivial preferred direction during isometric force exertion by lower limb. *J Neurophysiol* 93: 2614–2624, 2005. doi:10.1152/jn.00960.2004.
6. **van Zuylen EJ**, **Gielen CC**, **Denier van der Gon JJ.** Coordination and inhomogeneous activation of human arm muscles during isometric torques. *J Neurophysiol* 60: 1523–1548, 1988. doi:10.1152/jn.1988.60.5.1523.
7. **Voss H.** Tabelle der absoluten und relativen muskelspindelzahlen der menschlichen skelettmuskulatur [Tabulation of the absolute and relative muscular spindle numbers in human skeletal musculature]. *Anat Anz* 129: 562–572, 1971.
8. **Bergenheim M**, **Ribot-Ciscar E**, **Roll JP.** Proprioceptive population coding of two-dimensional limb movements in humans: I. Muscle spindle feedback during spatially oriented movements. *Exp Brain Res* 134: 301–310, 2000. doi:10.1007/s002210000471.
9. **Verschueren SM**, **Cordo PJ**, **Swinnen SP.** Representation of wrist joint kinematics by the ensemble of muscle spindles from synergistic muscles. *J Neurophysiol* 79: 2265–2276, 1998. doi:10.1152/jn.1998.79.5.2265.

10. **Scott SH**, **Loeb GE.** The computation of position sense from spindles in mono-and multiarticular muscles. *J Neurosci* 14: 7529–7540, 1994. doi:10.1523/JNEUROSCI.14-12-07529.1994.
11. **Smeets JB.** Bi-articular muscles and the accuracy of motor control. *Hum Mov Sci* 13: 587–600, 1994. doi:10.1016/0167-9457(94)90007-8.
12. **Sturnieks DL**, **Wright JR**, **Fitzpatrick RC.** Detection of simultaneous movement at two human arm joints. *J Physiol* 585: 833–842, 2007. doi:10.1113/jphysiol.2007.139089.
13. **Valbo AB.** Human muscle spindle discharge during isometric voluntary contractions. Amplitude relations between spindle frequency and torque. *Acta Physiol Scand* 90: 319–336, 1974. doi:10.1111/j.1748-1716.1974.tb05594.x.
14. **Hogg RV**, **Tanis EA.** *Probability and Statistical Inference*. New York: Macmillan, 1977.
15. **An KN**, **Hui FC**, **Morrey BF**, **Linscheid RL**, **Chao EY.** Muscles across the elbow joint: a biomechanical analysis. *J Biomech* 14: 659–669, 1981. doi:10.1016/0021-9290(81)90048-8.
16. **Bassett RW**, **Browne AD**, **Morrey BF**, **An KN.** Glenohumoral muscle force and moment mechanics in a position of shoulder instability. *J Biomech* 23: 405–415, 1990. doi:10.1016/0021-9290(90)90295-e.
17. **Langenderfer J**, **Jerabek SA**, **Thangamani VB**, **Kuhn JE**, **Hughes RE.** Musculoskeletal parameters of muscles crossing the shoulder and elbow and the effect of sarcomere length sample size on estimation of optimal muscle length. *Clin Biomech (Bristol, Avon)* 19: 644–670, 2004. doi:10.1016/j.clinbiomech.2004.04.009.
18. **Seireg A**, **Arvikar Rj.** *Biomechanical Analysis of Musculoskeletal Structure for Medicine and Sports*. New York: Hemisphere, 1989.
19. **Wood JE**, **Meek MG**, **Jacobsen SC.** Quantitation of human shoulder anatomy for prosthetic arm control. II. Anatomy matrices. *J Biomech* 22: 309–325, 1989. doi:10.1016/0021-9290(89)90045-6.
20. **Kuechle DK**, **Newman SR**, **Itoi E**, **Morrey BF**, **An KN.** Shoulder muscle moment arms during horizontal flexion and elevation. *J Shoulder Elbow Surg* 6: 429–439, 1997. doi:10.1016/s1058-2746(97)70049-1.
21. **Dukelow SP**, **Herter TM**, **Bagg SD**, **Scott SH.** The independence of deficits in position sense and visually guided reaching following stroke. *J NeuroEngineering Rehabil* 9: 72, 2012. doi:10.1186/1743-0003-9-72.
22. **Dukelow SP**, **Herter TM**, **Moore KD**, **Demers MJ**, **Glasgow JI**, **Bagg SD**, **Norman KE**, **Scott SH.** Quantitative assessment of limb position sense following stroke. *Neurorehabil Neural Repair* 24: 178–187, 2010. doi:10.1177/1545968309345267.
23. **Herter TM**, **Scott SH**, **Dukelow SP.** Systematic changes in position sense accompany normal aging across adulthood. *J Neuroeng Rehabil* 11: 43, 2014. doi:10.1186/1743-0003-11-43.
24. **Scott SH.** Apparatus for measuring and perturbing shoulder and elbow joint positions and torques during reaching. *J Neurosci Methods* 89: 119–127, 1999. doi:10.1016/s0165-0270(99)00053-9.
25. **Contu S**, **Hussain A**, **Kager S**, **Budhota A**, **Deshmukh VA**, **Kuah CW**, **Yam LH**, **Xiang L**, **Chua KS**, **Masia L**, **Campolo D.** Proprioceptive assessment in clinical settings: evaluation of joint position sense in upper limb post-stroke using a robotic manipulator. *PLoS One* 12: e0183257, 2017. doi:10.1371/journal.pone.0183257.
26. **Crowe A**, **Keessen W**, **Kuus W**, **van Vliet R**, **Zegeling A.** Proprioceptive accuracy in two dimensions. *Percept Mot Skills* 64: 831–846, 1987. doi:10.2466/pms.1987.64.3.831.
27. **Jones SA**, **Cressman EK**, **Henriques DY.** Proprioceptive localization of the left and right hands. *Exp Brain Res* 204: 373–383, 2010. doi:10.1007/s00221-009-2079-8.
28. **Kuling IA**, **Brenner E**, **Smeets JB.** Proprioceptive localization of the hand changes when skin stretch around the elbow is manipulated. *Front Psychol* 7: 1620, 2016. doi:10.3389/fpsyg.2016.01620.
29. **van Beers RJ**, **Sittig AC**, **Denier van der Gon JJ.** The precision of proprioceptive position sense. *Exp Brain Res* 122: 367–377, 1998. doi:10.1007/s002210050525.
30. **Wilson ET**, **Wong J**, **Gribble PL.** Mapping proprioception across a 2D horizontal workspace. *PLoS One* 5: e11851, 2010 [Erratum in *PLoS One* 5, 2010]. doi:10.1371/journal.pone.0011851.
31. **Brown LE**, **Rosenbaum DA**, **Sainburg RL.** Movement speed effects on limb position drift. *Exp Brain Res* 153: 266–274, 2003. doi:10.1007/s00221-003-1601-7.
32. **Smeets JB**, **van den Dobbelsteen JJ**, **de Grave DD**, **van Beers RJ**, **Brenner E.** Sensory integration does not lead to sensory calibration. *Proc Natl Acad Sci USA* 103: 18781–18786, 2006. doi:10.1073/pnas.0607687103.
33. **Wann JP**, **Ibrahim SF.** Does limb proprioception drift? *Exp Brain Res* 91: 162–166, 1992. doi:10.1007/BF00230024.
34. **Cleather DJ**, **Goodwin JE**, **Bull AM.** An optimization approach to inverse dynamics provides insight as to the function of the biarticular muscles during vertical jumping. *Ann Biomed Eng* 39: 147–160, 2011 [Erratum in *Ann Biomed Eng* 39: 2476-2478, 2011]. doi:10.1007/s10439-010-0161-9.
35. **Gregoire L**, **Veeger HE**, **Huijing PA**, **van Ingen Schenau GJ.** Role of mono- and biarticular muscles in explosive movements. *Int J Sports Med* 5: 301–305, 1984. doi:10.1055/s-2008-1025921.
36. **Heise G**, **Shinohara M**, **Binks L.** Biarticular leg muscles and links to running economy. *Int J Sports Med* 29: 688–691, 2008. doi:10.1055/s-2007-989372.
37. **Jacobs R**, **Bobbert MF**, **van Ingen Schenau GJ.** Mechanical output from individual muscles during explosive leg extensions: the role of biarticular muscles. *J Biomech* 29: 513–523, 1996. doi:10.1016/0021-9290(95)00067-4.
38. **Hoffman DS**, **Strick PL.** Step-tracking movements of the wrist. IV. Muscle activity associated with movements in different directions. *J Neurophysiol* 81: 319–333, 1999. doi:10.1152/jn.1999.81.1.319.
39. **Fagg AH**, **Shah A**, **Barto AG.** A computational model of muscle recruitment for wrist movements. *J Neurophysiol* 88: 3348–3358, 2002. doi:10.1152/jn.00621.2002.
40. **Herter TM**, **Kurtzer I**, **Cabel DW**, **Haunts KA**, **Scott SH.** Characterization of torque-related activity in primary motor cortex during a multi-joint postural task. *J Neurophysiol* 97: 2887–2899, 2007. doi:10.1152/jn.00757.2006.
41. **Lillicrap TP**, **Scott SH.** Preference distributions of primary motor cortex neurons reflect control solutions optimized for limb biomechanics. *Neuron* 77: 168–179, 2013. doi:10.1016/j.neuron.2012.10.041.
42. **Kistemaker DA**, **Van Soest AJ**, **Wong JD**, **Kurtzer I**, **Gribble PL.** Control of position and movement is simplified by combined muscle spindle and Golgi tendon organ feedback. *J Neurophysiol* 109: 1126–1139, 2013. doi:10.1152/jn.00751.2012.
43. **Cordo PJ**, **Horn JL**, **Künster D**, **Cherry A**, **Bratt A**, **Gurfinkel V.** Contributions of skin and muscle afferent input to movement sense in the human hand. *J Neurophysiol* 105: 1879–1888, 2011. doi:10.1152/jn.00201.2010.
44. **Edin BB**, **Johansson N.** Skin strain patterns provide kinaesthetic information to the human central nervous system. *J Physiol* 487: 243–251, 1995. doi:10.1113/jphysiol.1995.sp020875.
45. **Collins DF**, **Refshauge KM**, **Todd G**, **Gandevia SC.** Cutaneous receptors contribute to kinesthesia at the index finger, elbow, and knee. *J Neurophysiol* 94: 1699–1706, 2005. doi:10.1152/jn.00191.2005.
46. **Gandevia SC**, **McCloskey DI.** Joint sense, muscle sense, and their combination as position sense, measured at the distal interphalangeal joint of the middle finger. *J Physiol* 260: 387–407, 1976. doi:10.1113/jphysiol.1976.sp011521.
47. **Provins KA.** The effect of peripheral nerve block on the appreciation and execution of finger movements. *J Physiol* 143: 55–67, 1958. doi:10.1113/jphysiol.1958.sp006043.
48. **Refshauge KM**, **Kilbreath SL**, **Gandevia SC.** Movement detection at the distal joint of the human thumb and fingers. *Exp Brain Res* 122: 85–92, 1998. doi:10.1007/s002210050494.
49. **Clark FJ**, **Horch KW**, **Bach SM**, **Larson GF.** Contributions of cutaneous and joint receptors to static knee-position sense in man. *J Neurophysiol* 42: 877–878, 1979. doi:10.1152/jn.1979.42.3.877.
50. **Wang L**, **Millecchia R**, **Brown PB.** Correlation of peripheral innervation density and dorsal horn map scale. *J Neurophysiol* 78: 689–702, 1997. doi:10.1152/jn.1997.78.2.689.
51. **Goble DJ**, **Brown SH.** Task-dependent asymmetries in the utilization of proprioceptive feedback for goal-directed movement. *Exp Brain Res* 180: 693–704, 2007. doi:10.1007/s00221-007-0890-7.
52. **Darling WG.** Perception of forearm angles in 3-dimensional space. *Exp Brain Res* 87: 445–456, 1991. doi:10.1007/BF00231862.
53. **Gurari N**, **Drogos JM**, **Dewald JPA.** Individuals with chronic hemiparetic stroke can correctly match forearm positions within a single arm. *Clin Neurophysiol* 128: 18–30, 2017. doi:10.1016/j.clinph.2016.10.009.

54. **Tillery SI**, **Flanders M**, **Soechting JF.** A coordinate system for the synthesis of visual and kinesthetic information. *J Neurosci* 11: 770–778, 1991. doi:10.1523/JNEUROSCI.11-03-00770.1991.
55. **Soechting JF.** Does position sense at the elbow reflect a sense of elbow joint angle or one of limb orientation? *Brain Res* 248: 392–395, 1982. doi:10.1016/0006-8993(82)90601-1.
56. **Fuentes CT**, **Bastian AJ.** Where is your arm? Variations in proprioception across space and tasks. *J Neurophysiol* 103: 164–171, 2010. doi:10.1152/jn.00494.2009.
57. **Simo L**, **Botzer L**, **Ghez C**, **Scheidt RA.** A robotic test of proprioception within the hemiparetic arm post-stroke. *J Neuroeng Rehabil* 11: 77, 2014. doi:10.1186/1743-0003-11-77.
58. **Gandevia SC**, **Smith JL**, **Crawford M**, **Proske U**, **Taylor JL.** Motor commands contribute to human position sense. *J Physiol* 571: 703–710, 2006. doi:10.1113/jphysiol.2005.103093.
59. **Winter JA**, **Allen TJ**, **Proske U.** Muscle spindle signals combine with the sense of effort to indicate limb position. *J Physiol* 568: 1035–1046, 2005. doi:10.1113/jphysiol.2005.092619.
60. **Battaglia-Mayer A**, **Caminiti R**, **Lacquaniti F**, **Zago M.** Multiple levels of representation of reaching in the parieto-frontal network. *Cereb Cortex* 13: 1009–1022, 2003. doi:10.1093/cercor/13.10.1009.
61. **Soechting JF**, **Flanders M.** Moving in three-dimensional space: frames of reference, vectors, and coordinate systems. *Annu Rev Neurosci* 15: 167–191, 1992. doi:10.1146/annurev.ne.15.030192.001123.
62. **Scott SH.** Inconvenient truths about neural processing in primary motor cortex. *J Physiol* 586: 1217–1224, 2008. doi:10.1113/jphysiol.2007.146068.
63. **Smeets JB**, **Louw S.** The contribution of covariation to skill improvement is an ambiguous measure: comment on Müller and Sternad (2004). *J Exp Psychol Hum Percept Perform* 33: 246–249, 2007. doi:10.1037/0096-1523.33.1.246.
64. **Sternad D**, **Park SW**, **Müller H**, **Hogan N.** Coordinate dependence of variability analysis. *PLoS Comput Biol* 6: e1000751, 2010. doi:10.1371/journal.pcbi.1000751.
65. **Todorov E**, **Jordan MI.** Optimal feedback control as a theory of motor coordination. *Nat Neurosci* 5: 1226–1235, 2002. doi:10.1038/nn963.
66. **Gordon J**, **Ghilardi MF**, **Ghez C.** Accuracy of planar reaching movements. I. Independence of direction and extent variability. *Exp Brain Res* 99: 97–111, 1994. doi:10.1007/BF00241415.
67. **van Beers RJ**, **Haggard P**, **Wolpert DM.** The role of execution noise in movement variability. *J Neurophysiol* 91: 1050–1063, 2004. doi:10.1152/jn.00652.2003.